JOURNAL OF MATERIALS SCIENCE 21 (1986) 2049–2058

Instrumented impact testing of polyethersulphone

P. J. HINE, R. A. DUCKETT, I. M. WARD
Department of Physics, University of Leeds, Leeds LS2 9JT, UK

The impact behaviour of polyethersulphone has been studied using a specially constructed instrumented impact testing machine. This machine is of the pendulum type and the samples are fractured in three-point bend loading. It is shown that accurate force/deformation curves can be obtained, in spite of complications due to flexural vibrations of the test sample. Measurements were made on both sharp-notched and blunt-notched specimens over a range of crack lengths. It was found that the sharp-notched samples could be analysed in terms of fracture toughness, G_c, whereas the blunt-notched samples corresponded to a constant critical stress at the root of the notch. The importance of multiple crazes at the crack tip in blunt-notched specimens is emphasized. It is also shown that ageing reduces the fracture toughness, while on the other hand, the critical stress observed in blunt-notched specimens, which has been associated with the craze initiation stress, is not affected by ageing.

1. Introduction

Until recent developments a conventional Charpy or Izod impact test on polymers consisted of the measurement of the total energy required to break a notched or unnotched bar, and dividing this by the sample cross-sectional area to give an apparent fracture energy. It was shown by Brown [1] and Marshall *et al.* [2] that the impact fracture of sharply notched specimens could be more correctly analysed in terms of linear elastic fracture mechanics to determine the fracture toughness in terms of the critical strain energy release rate, G_c. It was shown that this method of analysis provided values for G_c which were independent of specimen geometry, and could be applied to several different polymer systems, even where mixed mode failure occurred [1–6]. In the case of blunt notched specimens it was later shown that the more appropriate measure of failure was the critical stress at the root of the notch, calculated from the measured stress at failure and the stress concentration factor for the geometry involved [5–7].

However, these two types of analysis depend on the measurement of only one parameter, the impact energy, and hence on the assumption that the material deforms in a linear elastic manner up to the point of fracture. It follows, therefore, that to extend the understanding of impact behaviour it is desirable to be able to measure the force on the sample during impact. This not only allows the force/deformation behaviour during impact to be ascertained, but also the force at failure which can lead to the determination of the critical stress intensity factor, K_c, a parameter uniquely related to G_c. This is in addition to the fracture energy which can now also be obtained by integration of the force/displacement curve.

A knowledge of the force/displacement curve is obviously most important in systems where the behaviour is complex. Instrumented impact techniques have been successfully used to examine the behaviour of semi-ductile polymers [8], glass fibre-reinforced plastics [9] and structural steels [10]. This paper describes the use of an instrumented Charpy type machine to study the impact properties of polyethersulphone. The aims of the work fall into two categories. Firstly the understanding of the complicated force/deformation behaviour measured under these dynamic conditions, and secondly a study of the effects of ageing on different types of polyethersulphone. This impact work forms part of an overall study which has been undertaken into the fracture properties of polyethersulphone. Previous work has looked at slow crack propagation in the double torsion test [11]; and the correlation between microscopic fracture properties as measured by an examination of the craze present at the crack tip, and microscopic fracture properties as measured by conventional fracture testing [12].

2. Experimental details

2.1. Materials

Two batches of polyethersulphone were available for testing, one moulded in 1974 and one moulded in 1979. The material in each case was grade P300 supplied in the form of 3 mm plaques, injection moulded by the Ministry of Defence from raw material produced by I.C.I. Limited. A complete range of impact tests was carried out in 1980 and 1984 on both types of material, so in all there are four groups of results covering various stages in the ageing process.

2.2. Specimens

Impact specimens were machined to be 8 mm × 80 mm and all were notched on one side. Firstly, to give sharp notches slots were cut and then a razor blade was sawn into the end of the slot. Secondly to produce blunt notches holes of the required radius were drilled in the correct position and were then carefully sawn into,

0022–2461/86 $03.00 + .12

care being taken not to disturb the opposite face of the hole. For the sharp-notched samples a range of crack lengths was examined whereas for the blunt-notched samples a standard crack length of 3.5 mm was used. Before testing, the crack length, a, and where appropriate the notch tip radius, ϱ, were measured using a travelling microscope.

2.3. Impact testing

The impact machine is a pendulum type employing three-point bend loading to break the sample. The machine was built from plans kindly supplied by BP Chemicals Ltd, with a number of extra modifications. These special features of the machine will now be discussed in greater detail.

2.3.1. Measurement of the angular position of the pendulum

This was accomplished in the original design by attaching to the main bearing of the pendulum a circular photographic negative, on which there were 2400 radial lines. As the pendulum rotated the lines interrupted a light beam and the pulses produced were counted by a photoelectric cell. By suitable triggering of the counter it was possible to measure both the initial drop height (and hence the impact velocity) and also the angle through which the pendulum moved after impact. From these measurements the energy absorbed on fracture was calculated.

2.3.2. Measurement of the force during impact

The force on the sample was determined using a strain gauge system. Initial attempts to attach strain gauges to the pendulum and also to the specimen supports produced a large amount of ringing on the final signal from the supporting members. The method finally chosen was to attach the strain gauges to steel rods which were mounted independently of the main base and formed the fixed supports for the specimen (Fig. 1). The semi-conductor strain gauges were glued on to a machined flat on the side of each rod. The system was calibrated under static force by applying a known force to the sample by means of a pulley system, and then measuring the output voltage.

2.3.3. Analysis of the force signal

After amplification by a wide band amplifier the output from the strain gauges was fed into a transient recorder. At its fastest this apparatus can store 1000 samples in 0.2 μsec. Most of the impact tests were carried out using a recording time of around 5 msec giving a typical resolution of 5 μsec. Having captured the fracture event it was then passed to an Acorn Atom microcomputer which could then display the resulting force/time curve. Analysis of this data, including integration to produce the stress/strain curve and the energy of fracture, could then be done at any subsequent convenient time. Hard copies of the results were also available using a printer. Finally each curve was also stored on floppy disk to enable further analysis at a later date.

It was possible to choose a range of drop heights for the pendulum and so give a range of impact velocities and hence different strain rates of testing. The range of linear impact velocities used was from 0.5 to 4 m sec^{-1}.

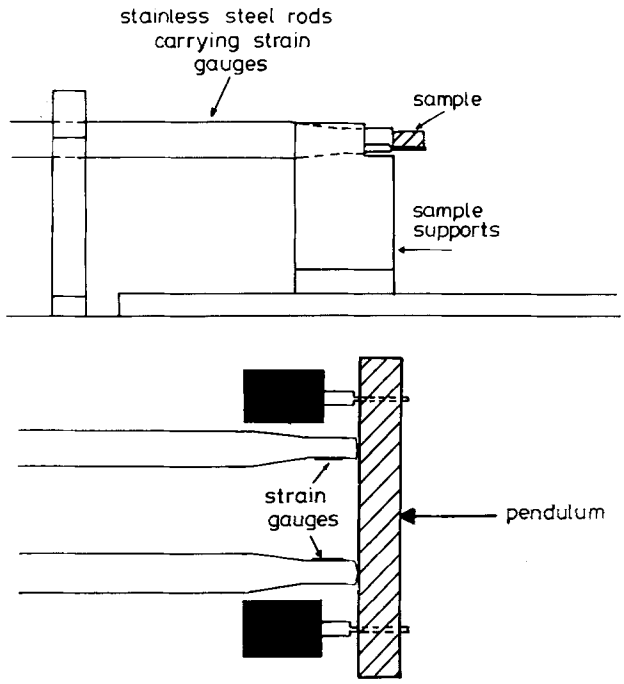

Figure 1 Sample position and force measurement for the instrumented impact machine.

3. Theory

There are two methods that can be applied to the analysis of a notched specimen at the point of fracture. The first, for sharp-notched samples, uses linear elastic fracture mechanics to calculate a value for the critical stress intensity factor, G_c. This analysis was first presented by Brown [1] and Marshall *et al.* [2] and is given by

$$G_c = \frac{U_0}{B}\frac{1}{C}\frac{dC}{da} \quad (1)$$

where U_0 is the energy stored in the sample at fracture, B the specimen thickness, and C the compliance of the specimen in terms of the crack length a, the form of which can be found in either [1] or [2].

Therefore knowing the energy absorbed on impact, U_0, and the specimen geometry, a value of G_c can be calculated. The impact energy was obtained by two methods, either by calculating the loss of potential energy of the pendulum on impact, or by integration of the force/time curve produced on failure. A more detailed discussion of these two methods can be found in a later section.

The second form of analysis, for blunt-notched samples, calculates the critical value of the maximum stress at the root of the notch on failure. This form of analysis was first developed by Fraser and Ward [3]. The maximum nominal stress, σ_n, for a specimen in elastic bending is given by

$$\sigma_n = \frac{6M_0}{B(W-a)^2} \quad (2)$$

where M_0 is the maximum bending moment, and W the specimen width. The maximum stress is then given

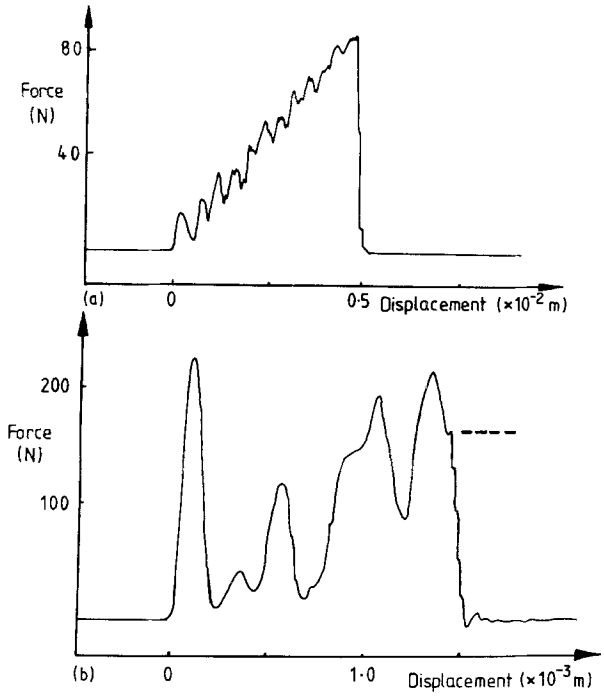

Figure 2 Force/displacement traces for a linear impact velocity of (a) 0.4 m sec^{-1} and (b) 3.5 m sec^{-1}.

by a product of the maximum nominal stress, σ_n, and the geometric stress concentration factor ε taken from Peterson [13].

In the past the value of M_0 at failure has been calculated from the absorbed energy assuming linear elasticity up to the point of failure. However, using the instrumented machine means that this assumption is no longer necessary: the true value of M_0, calculated from the fracture force, can be determined even when there is non-linear deformation before fracture occurs.

4. Results

4.1. Analysis of instrumented impact traces

Fig. 2 shows two typical force/displacement curves produced on impact. Fig. 2a was a sharp-notched sample impacted at a linear velocity of 0.4 m sec^{-1}. It can be seen that the force rises relatively smoothly although there is some oscillation of the signal around what would otherwise appear to be linear elastic deformation. The fracture force is quite distinct and after failure the force falls away rapidly to zero. Taken overall this is very close to a perfect representation of brittle failure.

Fig. 2b shows the force/displacement curve for a blunt notched sample impacted at a linear velocity of 3.5 m sec^{-1}. The rise of force on the sample with time for the faster impact velocity is now much harder to ascertain. This is because there are a number of effects which superimpose themselves on the deformation of the sample and these become more dominant at the higher strain rate.

Firstly there is the large initial peak, which in Fig. 2b is seen to be higher than the final fracture force. It has been shown by various authors [14–16] that this first peak is caused by inertial loading of the fixed supports as a result of decelerating the specimen after its first impact with the pendulum. The faster the impact velocity, the higher is this peak. It should be noted, however, that this is the force experienced by the specimen supports, and that the force experienced by the specimen is lower than this [14–16]. The time period (T) of this peak is dependent on the material properties [14]

$$T \propto \left(\frac{\text{density}}{\text{modulus}}\right)^{1/2} \tag{3}$$

and the specimen geometry, but independent of the loading conditions. So for similar specimen sizes this inertial peak should have the same time period independent of impact velocity. For PES, under the testing conditions employed, the inertial peak had a time period of about 120 μsec (cf. steel specimens of a similar size with a time period of 25 μsec [14]). Fortunately the fracture event for PES specimens occurs at a much longer time than this inertial period, although it is conceivable that for a very brittle material, and at a high impact velocity, that this inertial peak could mask the point of fracture.

After the inertial loading dies away the vibration of the specimen begins to affect the force trace. After impact the sample is free to vibrate in its natural modes, whilst also reacting to the pendulum. The vibration of the specimen is likely to be a combination of Modes I and III. These two individual modes of vibration are more clearly seen on a third force/displacement curve (Fig. 3). This shows a blunt-notched sample impacted at a linear velocity of 1 m sec^{-1}. Apart from the obvious fact that the deformation is no longer linear elastic up to fracture, it is also possible to see the two distinct modes of vibration. At the beginning of the trace, only the third order is visible, while at a later point when this has died away the longer vibration of the first order

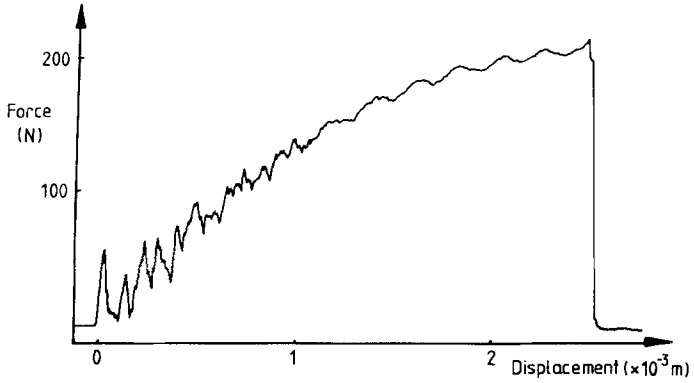

Figure 3 A typical impact trace showing the various contributions to the measured force/displacement behaviour.

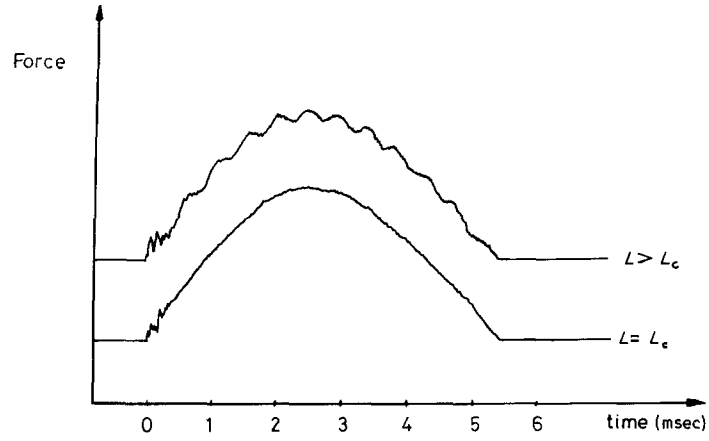

Figure 4 The effect on the measured force/displacement behaviour of changing the length of the sample.

becomes apparent. (For both Figs 2a and b fracture occurred before the third order vibration died away.) It is possible to effectively remove either of these modes of vibration. Beam theory [17] predicts the positions of the nodes for the various modes of vibration. By varying the length of the specimen it is possible to arrange for the nodes of vibration to occur at the force measuring points and so effectively remove them from the measured force/displacement trace. Fig. 4 shows the effect of such an experiment for a low blow test conducted on two specimens, one of which is the critical length, L_c, for the Mode I vibration and one which is longer than the critical length. It is seen that at the critical length the Mode I vibration ($\simeq 600\,\mu$sec) has effectively been removed from the force behaviour. However, at the beginning of each trace it is still possible to see the third order vibration ($\simeq 120\,\mu$sec). Although it is also theoretically possible to remove the third order vibrations this is impractical because a reasonable span between loading points would require a prohibitively long sample. This is unfortunate as it is this third order vibration which is the dominant factor over the time spans encountered up to fracture (Figs 2a and b).

From the considerations discussed above it can be concluded that the measured force/dispacement curve will be a combination of the actual deformation of the sample, inertial effects at the onset of impact and the various vibration modes of the specimen.

4.2. Instrumentation

Before the main programme of testing was undertaken it was necessary to check the calibration of the instrumentation. Firstly a comparison was made between the fracture energy as calculated from the loss of potential energy of the pendulum as previously described (Section 2.3.1) and the fracture energy obtained from the force/displacement curve measured on impact. This second quantity is calculated by a double integration given by

$$\text{Energy} = L \int_0^{t_f} F(t)\,\omega(t)\,dt \qquad (4)$$

where t_f is the time to fracture, $F(t)$ the force on sample at time t, L the length of the centre of percussion of the pendulum from the pivot, $\omega(t)$ the angular velocity at time t, and

$$\omega(t) = \frac{1}{ML} \int_0^{t_f} F(t)\,dt \qquad (5)$$

where M is the mass of the pendulum.

Good agreement was found between the energies calculated by these two different methods. (The energy obtained by the integration method was used for all subsequent calculations as at low drop angles the angular method tended to have more scatter due to the finite number of lines on the photographic negative (see Section 2.3.1).) This agreement between the two methods used to calculate the fracture energy was not confined to smooth force/displacement curves of which Fig. 2 is a good example. It also extended to curves where there was a more complicated loading cycle (Fig. 2b) as experienced at higher loading rates.

A second check on the instrumentation was carried out by comparing the fracture force for a sample which behaved in a linear elastic manner, with the fracture force, P_f, predicted for the sample from the measured fracture energy, U_0, and the calculated specimen compliance, C, given by

$$P_f = \left(\frac{2U_0}{C}\right)^{1/2} \qquad (6)$$

This again showed good agreement between the measured and the calculated fracture forces. An especially interesting result was found for the higher strain-rate tests. Consider again Fig. 2b and notice the dotted line which represents the fracture force as predicted by the integrated energy and the calculated compliance. It is seen that this line is close to the point of fracture and not the maximum force.

4.3. Impact testing of PES

As previously explained, tests were carried out on sharp- and blunt-notched specimens for the two different materials tested in 1980 and 1984. To reduce the discussion to manageable proportions, in most cases an example of only one type of material is quoted for each type of test carried out.

4.3.1. Sharp-notched samples

A range of crack length, a, to sample width, W, ratios were examined for each sample group. All the

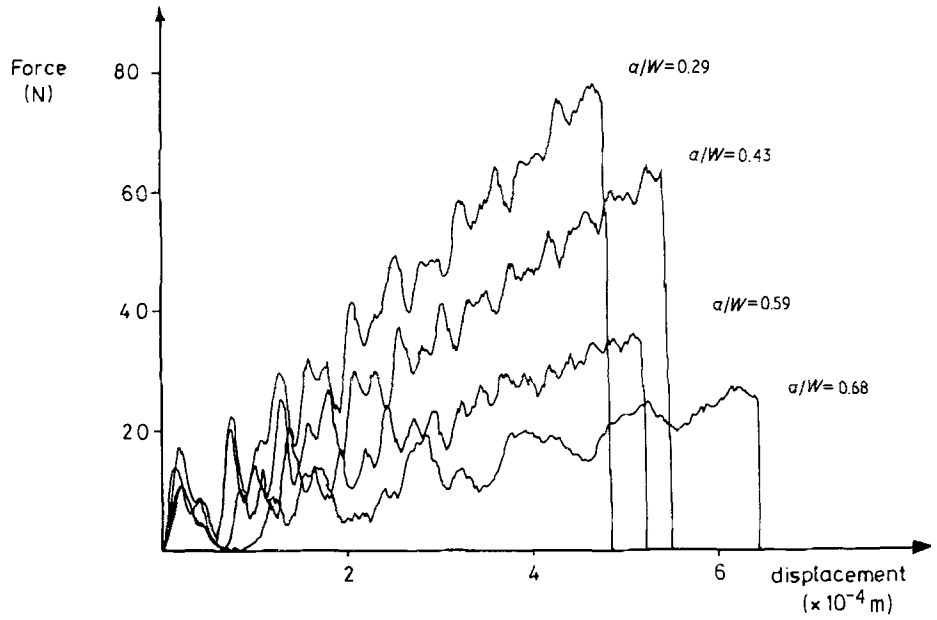

Figure 5 Force/displacement traces for sharp-notched samples, moulded in 1974 and tested in 1984, with different crack lengths.

sharp-notched tests were conducted at an impact velocity of 0.4 m sec^{-1} (corresponding to a nominal strain rate of around 6 sec^{-1}). Fig. 5 shows a set of force/displacement curves for such a group of samples with a range of a/W, in this case for the material moulded in 1974 and tested in 1984. The various features of such curves, previously discussed, can be found on the diagram. Note that for the longest crack lengths the force variation, caused by vibration of the sample, is a large proportion of the fracture force. It can be seen that the deformation is linear elastic up to failure and that after the point of fracture the force drops rapidly to zero, indicating brittle failure. This is borne out by the fracture surfaces which show the smooth surface indicative of such a failure mode. After integration of the curves to produce the energy absorbed on fracture, U_0, the samples are analysed using Equation 1, by plotting U_0 against the geometric factor BC (da/dC). The gradient of such a plot gives the critical value of the strain energy release rate, G_c. An example of such a plot, in this case for the material moulded in 1979 and tested in 1980, is shown in Fig. 6. The straight line plot shows that the value of G_c is independent of crack length and so is a good material parameter. This was found for all four groups of samples, as was the linear elastic deformation behaviour previously described. The positive intercept on the energy axis is a measure of the kinetic energy lost on accelerating the sample from rest and has been reported many times before (e.g. [2, 3, 5]). A summary of the results from the four groups of samples tested with sharp notches is shown in Table I.

4.3.2. Blunt-notched samples

All the blunt-notch samples were tested at an impact velocity of 1 m sec^{-1} (corresponding to a nominal

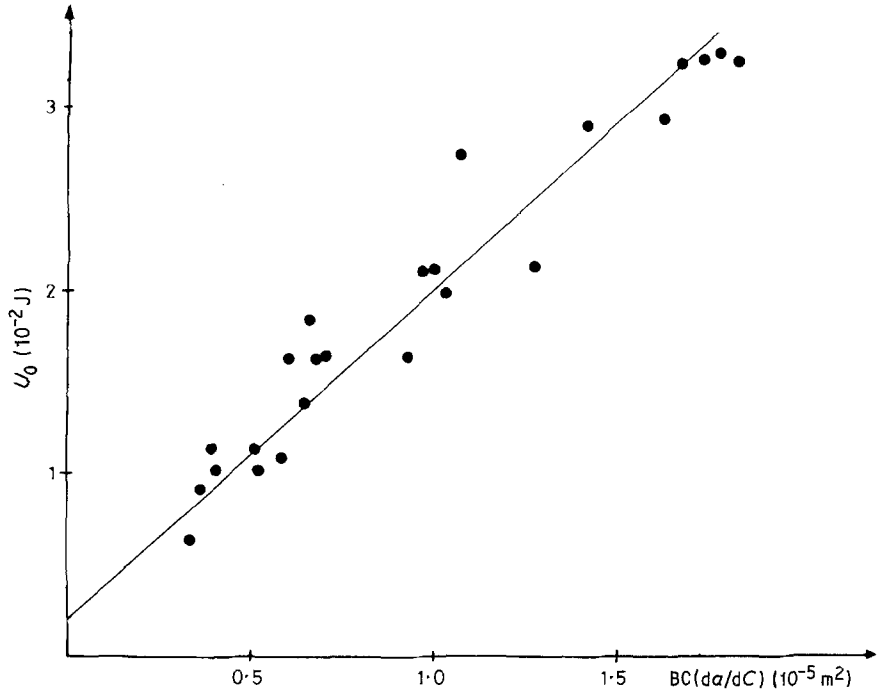

Figure 6 Fracture energy, U_0 against the geometric factor BC (da/dC) for sharp notched samples of the material moulded in 1979 and tested in 1983.

TABLE I Values for the critical strain energy release rate, G_c (kJ m^{-2}) for sharp-notched samples

	Moulded in 1974	Moulded in 1979
Tested in 1980	2.27 ± 0.30*	1.81 ± 0.30
Tested in 1984	1.68 ± 0.25	1.44 ± 0.21

*All the errors quoted refer to 95% confidence limits.

TABLE II Values for the maximum stress, σ_m (MN m^{-2}) for blunt-notched samples

	Moulded in 1974	Moulded in 1979
Tested in 1980	260 ± 10* 335 ± 40†	390 ± 30*
Tested in 1984	255 ± 15* 330 ± 50†	380 ± 25*

*Single crack propagation.
†Multiple crack propagation.

strain rate of 20 sec^{-1}). A series of force/displacement curves for a range of notch tip radii is shown in Fig. 7, in this case for the material moulded in 1979 and tested in 1984. The first observation is that the deformation is no longer linear elastic up to the point of fracture, although examination of the fracture surfaces after failure still indicates brittle fracture occurring with no evidence of any mixed mode failure (e.g. shear lips). If, as under normal circumstances, the maximum stress at the root of the notch were to be calculated from the energy absorbed on failure and assuming linear elastic behaviour, then an abnormally high value would be obtained due to this wrong assumption. The measurement of the force/displacement curve is obviously important for this sort of deformation behaviour. It is seen from Fig. 7 that the force, and hence the nominal stress on the sample at fracture, rises with increasing notch tip radius. However, if the force/displacement curves are transformed to show the maximum stress at the notch tip during impact, calculated from Equation 2, then a different picture emerges. Fig. 8 shows such a representation for the same group of samples as shown in Fig. 7, and it is seen that the maximum stress at the notch tip at failure is now independent of notch tip radius. This parameter therefore proves to be a much better representation of the material properties under these blunt-notch conditions, rather than the calculation of a value for G_c which was found to rise significantly with increasing notch tip radius. An alternative presentation for these results is to plot the nominal stress at fracture against the reciprocal of the stress concentration factor. Fig. 9 shows such a plot and as expected a very good linear relationship is seen. The slope of this line then gives the maximum stress at fracture. For the material moulded in 1979 it was found that the maximum stress had a similar value when tested in 1980 and in 1984 at around 380 MN m^{-2}.

This constant value for the maximum stress was, however, not true for the material moulded in 1974. When tested, both in 1980 and 1984, it was found that there was a range of values for the maximum stress. Fig. 10 shows the results for the material moulded in 1974 and tested in 1984 plotted as nominal stress against the reciprocal of the stress concentration factor. It is obvious that there is no longer the linear relationship that was evident for the 1979 material. However, examination of the samples after fracture did produce an interesting fact. All the samples on the line shown (■) exhibited a clean smooth fracture occurring through one crack. However, all the samples above this line (●) showed multiple cracking around the notch tip, in some cases with the sample splitting into three or more separate pieces on fracture. Examples of single and multiple fractures are shown in Fig. 11. A summary of the results obtained from the blunt notched samples is shown in Table II.

5. Discussion

5.1. Sharp-notched samples

The measurement of the force on the sample proved very useful in assessing the force/deformation behaviour of the material under impact. For the sharp-notched samples it was found in all cases that the material behaved in a linear elastic manner up to the point of failure, bearing out the assumption that it is permissible to use linear elastic fracture mechanics to analyse the results. In all cases the failure was unstable once crack initiation had occurred, and no evidence could be found either on the force/displacement curves, or on the fracture surfaces, for any regions of slow crack growth. How the value of G_c calculated under impact conditions compared with results from other fracture tests performed on the same material [11, 12] can be seen in Table III, specifically for the 1979 material tested in 1980. It is seen that there is an increase in G_c with strain rate of testing and hence

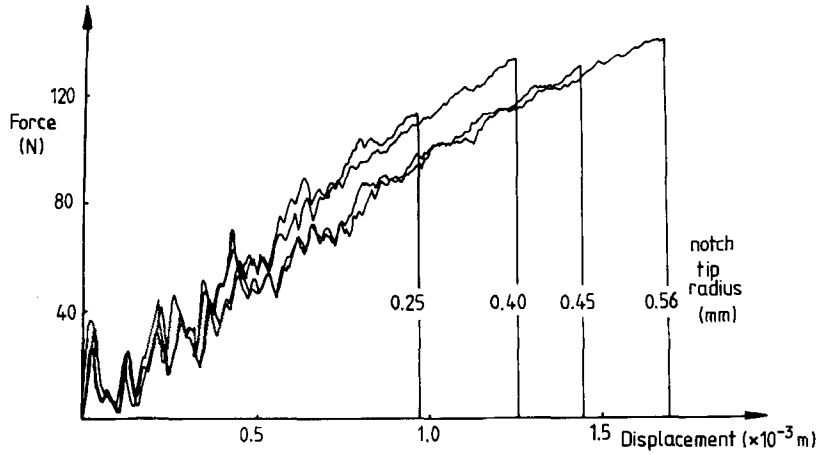

Figure 7 Force/displacement traces for blunt notched samples of the material moulded in 1979 and tested in 1980.

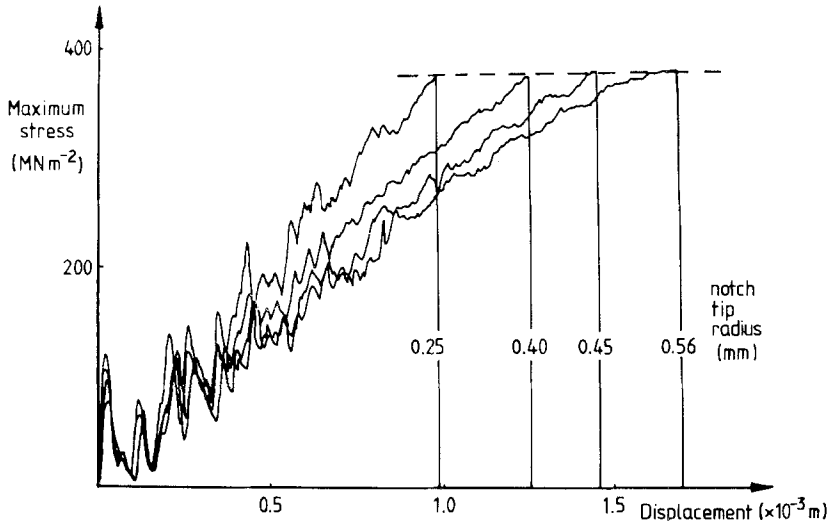

Figure 8 Maximum stress against displacement for blunt notched samples of the material moulded in 1979 and tested in 1980 (as for Fig. 7).

crack speed, although some care has to be taken with this sort of comparison. For the compact tension and double torsion tests the mode of crack propagation tends to be stable; once initiated the crack needs further input of energy to propagate it across the sample. It was seen in these tests that the presence of a craze in front of a propagating crack was important in determining the fracture properties of PES. The values of G_c calculated from analysing this stable form of propagation reflects the influence of the craze on the fracture behaviour and is independent of the initial notching procedure. For the impact test, which was found to be an unstable test, the energy absorbed on impact is dominated by the notching procedure. For the razor-notched samples a craze is present at the crack tip and so the value of G_c measured is related to the propagation of the crack and craze. However, for the blunt-notched samples a higher apparent value of G_c is measured, which includes a component associated with initiation of the craze as well as propagation. Under these conditions the calculation of a maximum critical stress provides a better critical parameter.

The results in Table I show that the value of G_c falls with ageing for both types of material. Although the two materials are nominally the same grade, it is more likely that there are some differences between them and that a direct comparison is unwise. In particular, the storage history of the 1974 material, between moulding and receiving it in 1979, is unknown. Furthermore, no attempt was made to assess the affect of water content on the fracture behaviour. So although no direct comparison can be made between the two materials, it has proved useful to be able to test and analyse both in order to obtain a further understanding of the impact properties of PES. The fall of G_c with ageing, as seen for both materials is not unexpected. Struick [18] has presented results for the effect of ageing on the Charpy impact strength of a number of polymers with different mechanical properties. He concluded that the effect of ageing, via a decrease in the free volume, would be more apparent the greater the ductility of the polymer. Thus the impact strength of PMMA was found to be unaffected by changes in the free volume, that is on ageing. Hence for a ductile polymer like PES it would be expected that the impact strength would fall with time.

TABLE III The value of the critical strain energy release rate, G_c (kJ m^{-2}) for various tests methods for the material moulded in 1979 and tested in 1980

Compact tension/craze shape	0.47 ± 0.02
Double torsion	0.70 ± 0.05
Three-point impact	1.81 ± 0.30

5.2. Blunt-notched samples

For the blunt-notched samples it was found that the size of the notch affected the deformation behaviour and also that the two materials differed markedly in their fracture behaviour. The material was found to change from linear elastic behaviour for low notch tip radii to a mixture of elastic and plastic behaviour for larger notch tip radii. The measurement of the force on the sample was very useful in examining these differences in deformation behaviour. For the 1979 material it was found that although G_c was dependent on specimen geometry the calculation of a maximum stress provided a geometry-independent material property. Again unstable failure, through a single crack, was seen in all cases but this is hardly surprising as with a blunt notch no craze is present on loading. On the assumption that the energy to propagate a

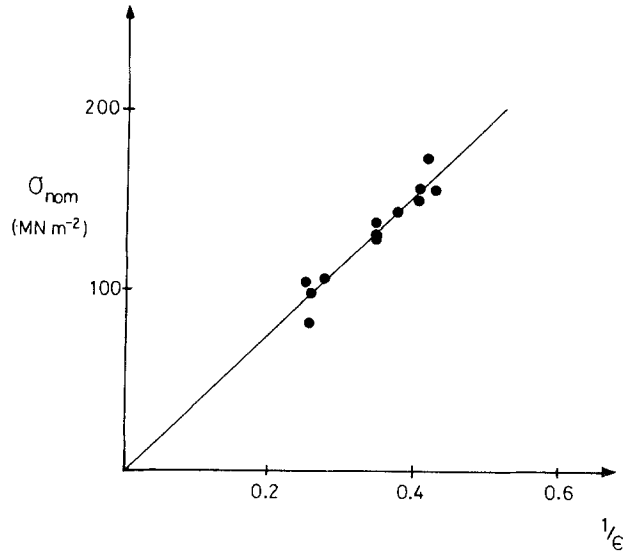

Figure 9 Nominal stress against the reciprocal of the stress concentration factor for blunt-notched samples of the material moulded in 1979 and tested in 1980 (as for Figs 7 and 8).

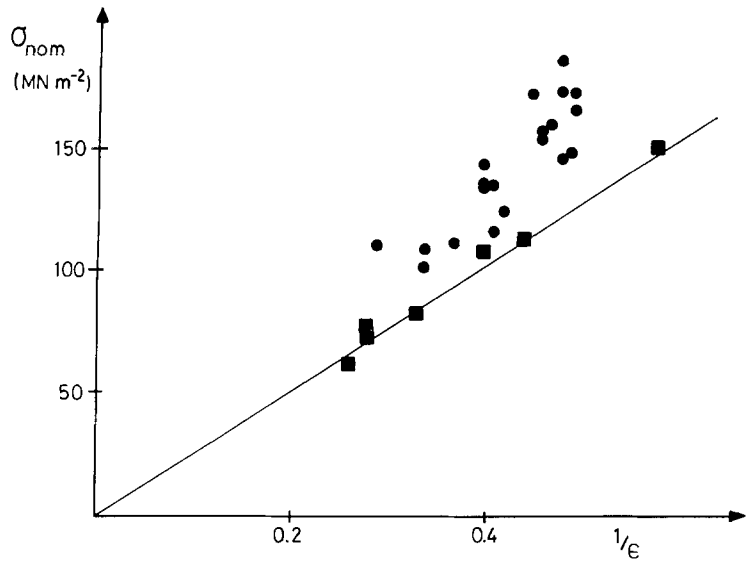

Figure 10 Nominal stress against the reciprocal of the stress concentration factor for blunt-notched samples of the material moulded in 1974 and tested in 1984. (■) Single crack propagation, (●) multiple cracking.

craze is less than that to initiate a craze unstable failure will always occur after initiation. For the 1974 material the situation was not so simple with single and multiple cracking occurring. Studies of multiple cracking, for instance by Congleton and Petch [19] and Anthony and Congleton [20] have suggested that this type of behaviour occurs due to microcracks nucleating in front of an advancing crack so causing the crack to branch. One possible mechanism for this to occur in polymers is through multiple crazing. A typical picture of the craze present at the tip of a crack in the 1974 material (Fig. 12) produced using reflected monochromatic light, shows a complicated interference pattern with Moiré fringes present and generally is in contrast to the clear interference fringes seen when viewing a craze in the 1979 material [11, 12]. This type of interference pattern, as seen in the 1974 material, has been attributed by Schirrer and Goett [21] to the existence of multiple crazing. This then explains the different behaviour of the 1974 and 1979 materials under blunt notch conditions, i.e. the multiple crazing in the 1974 material causes multiple cracking to occur. The driving force for multiple cracking will be the amount of stored energy available for initiation. For sharp-notched samples and low notch tip radii there is probably not enough stored energy for multiple cracking and so single cracking occurs, whereas for the larger notch tip radii there is much more stored energy available on initiation and so multiple cracking can occur through the multiple crazes present. Furthermore, the theories of multiple cracking previously mentioned [19, 20] show that for this mode of failure it is likely that the value of G_c (or K_c) will be greater, by a certain factor, than the G_c measured for single crack propagation. This then explains why the values of σ_{nom} (or G_c) are greater in the case of multiple cracking than for single crack propagation (Fig. 10).

In the previous section it was suggested that the fall in the values of G_c for sharp notches, between being tested in 1980 and 1984, was due to the effects of ageing. However, ageing tends to be relatively rapid

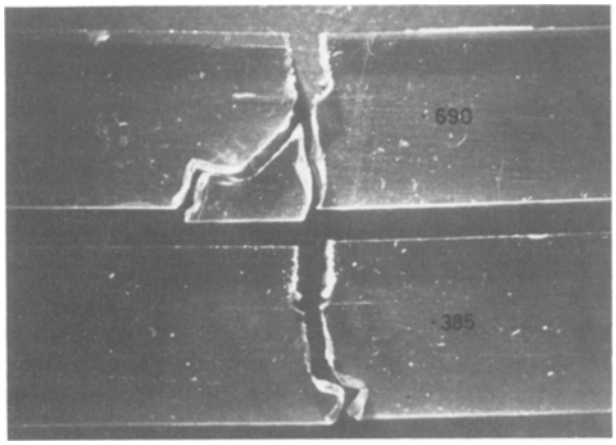

Figure 11 Single and multiple fracture for the material moulded in 1974 and tested in 1984.

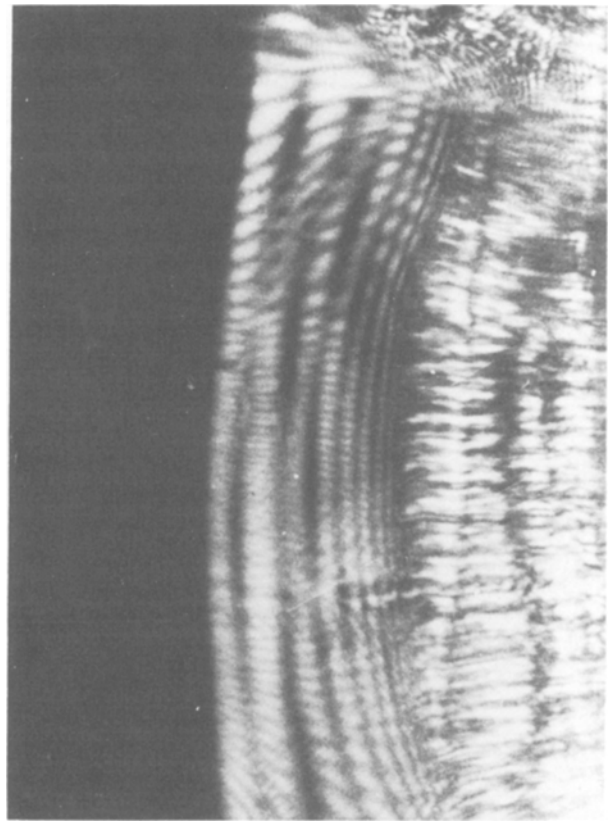

Figure 12 A typical interference pattern produced from a craze present at the crack tip of the material moulded in 1974.

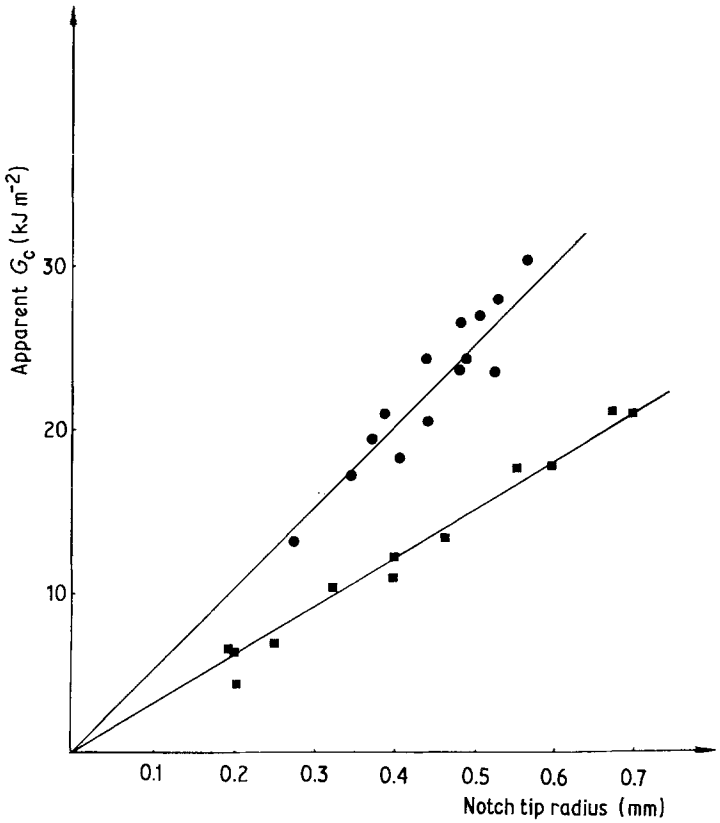

Figure 13 Apparent G_c against notch tip radius, ϱ, for the material moulded in 1974. (●) Tested in 1980, (■) tested in 1984.

immediately after moulding and then tends to slow down as time passes. This suggests that for the sample moulded in 1974, the value of G_c for the newly moulded material would be very high. It has been seen that the 1974 material shows evidence of multiple crazing present at the crack tip as opposed to a single craze present in the 1979 material. This multiple crazing, could, on loading, lead to a degree of crack blunting and so raise the measured value of G_c for the 1974 material from that seen in the singly crazed 1979 material. This suggests that the implied high value of G_c for the newly moulded 1974 material (Table II) could be due to the contribution of multiple crazing in raising the effective G_c.

The results from the blunt notched tests for the maximum stress as shown in Table II, seem to contradict the fall of G_c with ageing (Table I) by suggesting no effect due to crazing. This is a slightly false picture as the plot of apparent G_c against notch tip radii for the 1979 material tested in both 1980 and 1984 shows (Fig. 13). It can be seen that the value of apparent G_c, dependent on the energy absorbed in the sample at failure, still falls with ageing which is consistent with the sharp notch results. This result is mainly due to a fall in the extension to break (or a loss of ductility) of the material on ageing whilst the stress at break remains relatively independent of ageing. This is reflected by the fact that the maximum stress is unaffected by the ageing process whereas the critical strain energy release rate G_c falls. It seems, therefore, that for polyethersulphone any conclusion regarding the effect of ageing on the fracture behaviour is sensitive to the choice of the particular parameter determined for examination.

6. Conclusions

It has been shown that an instrumented impact machine is very useful in understanding impact properties, especially for examining the force/deformation behaviour during impact and is essential for deciding which method of analysis should be applied. Although fairly complicated, under these dynamic conditions, the various contributions to the measured force/deformation behaviour have been analysed and explained.

Sharp-notched samples of polyethersulphone were shown in impact testing to exhibit purely linear elastic behaviour up to the point of fracture whereas blunt-notched samples were shown to exhibit a mixture of elastic and plastic deformation behaviour. The differences between the two types of material tested, in terms of single or multiple crack propagation, were shown to depend on the presence of either single or multiple crazes at the crack tip and also the amount of stored elastic energy in the system at crack initiation. Finally, the assessment of the effect of ageing was dependent on the choice of fracture parameter determined. In particular, the critical strain energy release rate, G_c, fell with ageing, whereas the maximum stress at fracture was independent of ageing. It can be concluded that the stress to initiate crazing is comparatively insensitive to ageing whereas the fracture toughness which depends on the extensibility of the polymer is very dependent on ageing.

References

1. H. R. BROWN, *J. Mater. Sci.* **8** (1973) 941.
2. G. P. MARSHALL, J. G. WILLIAMS and C. E. TURNER, *ibid.* **8** (1973) 949.
3. R. A. FRASER and I. M. WARD, *ibid.* **9** (1974) 1624.
4. E. PLATI and J. G. WILLIAMS, *Polym. Eng. Sci.* **15** (1975) 470.
5. R. A. FRASER and I. M. WARD, *J. Mater. Sci.* **12** (1977) 459.
6. G. L. PITMAN, I. M. WARD and R. A. DUCKETT, *ibid.* **13** (1978) 2092.

7. H. R. BROWN and I. M. WARD, *ibid.* **8** (1973) 1365.
8. F. X. de CHARENTENARY, J. J. ROBIN and T. VU-KHANH, Conference on "Deformation, Yield and Fracture of Polymers", (Plastics and Rubber Institute, London, 1982).
9. G. E. OWEN Jr, *Polym. Eng. Sci.* **21** (1981) 8.
10. G. D. FEARNEHOUGH, Conference on "Dynamic Crack Propagation" (Nordhoff, Leyden, 1972) p. 77.
11. P. J. HINE, R. A. DUCKETT and I. M. WARD, *J. Mater. Sci.* **19** (1984) 3796.
12. *Idem, Polymer* **22** (1981) 1745.
13. R. E. PETERSON, "Stress Concentration Factors" (Wiley, New York, 1953).
14. C. E. TURNER, "Impact Testing of Metals", ASTM STP 466 (American Society for Testing and Materials, Philadelphia, Pennsylvania, 1970) p. 93.
15. S. VENZI, A. H. PRIEST and M. J. MAY, "Impact Testing of Metals", ASTM STP 466 (American Society for Testing and Materials, Philadelphia, Pennsylvania, 1970) p. 165.
16. D. R. IRELAND, "Instrumental Impact Testing", ASTM STP 563 (American Society for Testing and Materials, Philadelphia, Pennsylvania, 1974) p. 3.
17. B. E. READ and G. D. DEAN, "The Determination of Dynamic Properties of Polymers and Composites" (Adam Hilger, Bristol, 1978).
18. L. C. E. STRUICK, "Physical Ageing in Amorphous Polymers and Other Materials" (Elsevier, Amsterdam, 1978).
19. J. CONGLETON and N. J. PETCH, *Phil. Mag.* **16** (1967) 749.
20. S. R. ANTHONY and J. CONGLETON, *Met. Sci. J.* **2** (1968) 158.
21. R. SCHIRRER and C. GOETT, *J. Mater. Sci.* **16** (1981) 2563.

Received 21 February
and accepted 14 August 1985